IUBMB *Life*, 61(11): 1029–1042, November 2009

Critical Review

Fluorescent Proteins for Live Cell Imaging: Opportunities, Limitations, and Challenges

Jörg Wiedenmann[1], Franz Oswald[2] and Gerd Ulrich Nienhaus[3,4,5]
[1]*National Oceanography Centre, University of Southampton, Southampton, UK*
[2]*Department of Internal Medicine I, University of Ulm, Ulm, Germany*
[3]*Institute of Applied Physics and Center for Functional Nanostructures, University of Karlsruhe, Karlsruhe, Germany*
[4]*Institute of Biophysics, University of Ulm, Ulm, Germany*
[5]*Department of Physics, University of Illinois at Urbana-Champaign, Urbana, IL, USA*

Summary

The green fluorescent protein (GFP) from the jellyfish *Aequorea victoria* can be used as a genetically encoded fluorescence marker due to its autocatalytic formation of the chromophore. In recent years, numerous GFP-like proteins with emission colors ranging from cyan to red were discovered in marine organisms. Their diverse molecular properties enabled novel approaches in live cell imaging but also impose certain limitations on their applicability as markers. In this review, we give an overview of key structural and functional properties of fluorescent proteins that should be considered when selecting a marker protein for a particular application and also discuss challenges that lie ahead in the further optimization of the glowing probes.

IUBMB *Life*, 61(11): 1029–1042, 2009

Keywords live cell imaging; coral fluorescent proteins; GFP; RFP; monomeric red fluorescent protein; far red fluorescent protein; photoconversion; photoactivation; super resolution microscopy.

INTRODUCTION

The green fluorescent protein (GFP) was discovered in the course of bioluminescence studies of the hydrozoan jellyfish *A. victoria* (*1*). The 28-kDa protein emits bright green light upon stimulation with UV or blue light (*2*). Its primary structure was elucidated in 1992 by Prasher et al. (*3*). The functional expression in recombinant systems revealed the revolutionary potential of GFP as a genetically encoded fluorescence marker (*4*). Such an application was enabled by the autocatalytic formation of the 4-(*p*-hydroxybenzylidene)-5-imidazolinone (*p*-HBI) chromophore from the amino acid triplet Ser-Tyr-Gly in the center of an 11-stranded β-barrel (*5*). Since then, GFP was used as a marker of gene activity and to label proteins and subcellular compartments within living cells. Further applications included tracking of GFP labeled cells in tissues and the use in numerous GFP-based sensor applications (*5–8*). Mutagenesis yielded GFP derivatives with blue- and yellow-shifted fluorescence and variants with optimized properties for cell biological experimentation that allowed several processes to be studied in parallel (*5, 8-10*). The tremendous impact of GFP technology on life sciences research was acknowledged by awarding the nobel prize of chemistry 2008 to Osamu Shimomura, Martin Chalfie and Roger Tsien for the "discovery and development of the green fluorescent protein, GFP" (*11*). However, efforts to create dearly needed red emitting variants by engineering of GFP were unsuccessful during the first years of research on fluorescent proteins (*12*). Naturally occurring red fluorescent GFP-like proteins were discovered in sea anemones (*13*). Shortly thereafter, the first genes of GFP-like proteins, including the red emitter dsRed, were isolated from different anthozoa species (*14–16*). Characterization of the novel proteins revealed that more than 700 million years of molecular evolution created diverse properties with exciting application potential, including an entire rainbow of fluorescence colors and the possibility to control the emission intensity or color by targeted light irradiation (*8, 17–20*). Unfortunately, adverse properties such as oligomerization or slow maturation may hamper the use of these proteins in some applications (*16*). In this review, we summarize biochemical and photophysical properties of GFP-like proteins and their relevance for imaging applications as well as prospects for their further optimization.

Received 14 July 2009; accepted 5 August 2009
Address correspondence to: Jörg Wiedenmann University of Southampton, National Oceanography Centre, Southampton SO14 3ZH, UK. Tel: +44 (0)23 8059 6497. Fax: +44 (0)23 8059 3052.
E-mail: joerg.wiedenmann@noc.soton.ac.uk

ISSN 1521-6543 print/ISSN 1521-6551 online
DOI: 10.1002/iub.256

Table 1
Properties of FPs emitting in the orange-red spectral range

FP variant	Oligomerization degree (no. of protomers)	Excitation maximum (nm)	Emission maximum (nm)	Stokes_ shift	QY	E_{mol} (M^{-1} cm^{-1})	Relative brightness[a] (% of EGFP)	$t_{0.5}$ maturation at 37°C (h)
EGFP (*35*)	1	488	507	19	0.6	53,000[b]	100	–
mKO2 (*36*)	1	551	565	14	0.62	63,800[b]	124	–
td-Tomato (*25*)	2	554	581	27	0.69	69,000	150	1
mOrange2 (*37*)	1	549	565	16	0.60	58,000[c]	109	4.5
TurboRFP (*38*)	2	553	574	21	0.67	92,000[c]	194	–
TagRFP-T (*37*)	1	555	584	29	0.41	81,000[c]	104	1.66
mRuby (*39*)	1	558	605	47	0.35	not applicable[c] 112,000[d]	123	2.8
DsRedExpress2 (*40*)	4	554	591	37	0.42	35,600	47	0.7
eqFP611 (*16*)	4	559	611	52	0.45	116,000[c] 146,000[d]	164[c]	not applicable
mCherry (*25*)	1	587	615	28	0.22	72,000[c]	50	0.25 [0.6 (*40*)]
mKeima (*41*)	1	440	620	180	0.24	14,400[b]	11	–
mRaspberry (*26*)	1	598	625	27	0.15	86,000[c]	41	0.92
RFP630 (*24*)	4	583	630	47	0.35	50,000[c]	55	not applicable
mKate2 (*42*)	1	588	635	47	0.4	62,500[c]	79	~0.33
Katushka (*27*)	2	588	635	47	0.34	65,000[c]	70	0.33
RFP637 (*24*)	4	587	637	50	0.23	72,000[c] 141,300[d]	52[c] 102[d]	<8[e]
RFP639 (*24*)	4	588	639	51	0.18	69,000[c] 110,400[d]	39[c] 63[d]	1.5
hcRed (*43*)	2	594	645	51	0.05	70,000[c]	11	–
mPlum (*26*)	1	590	649	59	0.1	41,000[c] 143,400[d,f]	13[c] 45[d]	1.66
AQ14 (*44*)	4	595	663	68	–	–	–	–

[a]Product of QY and E_{mol} of purified proteins compared to the brightness of EGFP (53,000 M^{-1} cm^{-1} × 0.60).
[b]Concentration of the red chromophore deduced from the protein concentration as determined by colorimetric methods.
[c]Concentration of the red chromophore determined by the alkaline denaturation method (*45*).
[d]Concentration of the red chromophore determined by the dynamic difference method (*24*).
[e]Determined from expression in HEK293 cells.
[f]Values from ref. (*24*).

MODIFICATIONS OF THE GFP CHROMOPHORE AND ITS ENVIRONMENT PRODUCE A RAINBOW OF PROTEIN COLORS

Natural sources including corals, sea anemones, hydrozoans, crustaceans and even basic chordate animals yielded GFP-like proteins with emission colors ranging from cyan to red (*19, 21, 22*). Molecular phylogeny showed that the colors evolved from a single, most likely green fluorescent ancestral protein by variation of the *p*-HBI chromophore (*19, 23*). The color palette was extended considerably, especially toward the far-red end of the spectrum by protein engineering (Table 1) (*24–27*). The chromophore structures and fluorescence spectra of the major color classes are shown in Fig. 1. Cyan fluorescent proteins such as asFP499 are frequently found in reef building corals and sea anemones (*19, 28, 29*). They feature the chemically unaltered *p*-HBI chromophore of GFP. Polar interactions of the chromophore and its surrounding residues affect the charge distributions in the ground and electronically excited states and result in blue shifted emission (*29-32*). The yellow emission of zFP538 from *Zoanthus* sp. can be attributed to an N-terminal carboxamide that extends the conjugated *p*-HBI π-electron system as a result of the cleavage of the peptide backbone upon formation of a third heterocycle (*33*). Alternatively, the yellow fluorescence of naturally occurring FPs such as phiYFP can result from an extension of the conjugated π-electron system via π-stacking interactions of the hydroxyphenyl ring of the chromophore-forming tyrosine and another aromatic amino acid (*17*). Interestingly, the same mechanism is responsible for the bathochromic shift in GFP variants obtained by mutagenesis (*34*).

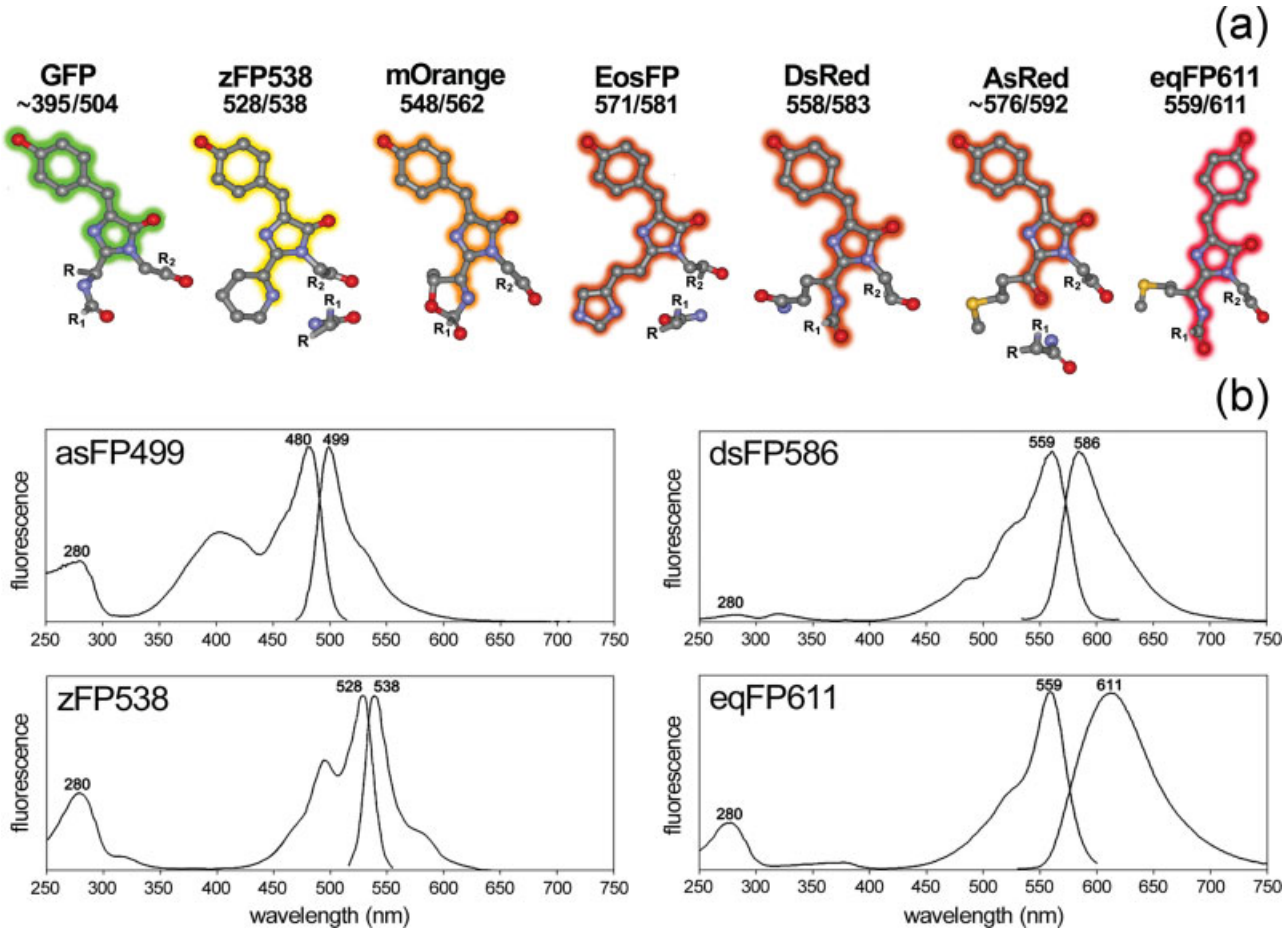

Figure 1. Structural depictions of the *p*-HBI chromophore and its derivatives as ball and stick models (atom color coding: grey = carbon, red = oxygen, blue = nitrogen, yellow = sulfur; $R/R_1/R_2$ symbolize protein rests) (a). The wavelengths of the excitation and emission maxima are given below the protein names. The fluorescence color is symbolized by colored underlays highlighting the conjugated π-systems. Selected fluorescence spectra of GFP-like proteins covering the emission range from cyan to red (b), peak positions in nm are included. Figure modified from ref. (*20*). Copyright 2009 Wiley-VCH Verlag GmbH& Co. KGaA, Weinheim, reproduced with permission.

Fragmentation of the peptide backbone is involved in the formation of a carbonyl group that becomes part of the red emitting chromophore of asRed (asFP595 A143S) (*46-49*). The red-shifted emission of the dsRed variant mOrange results from the formation of an oxazole heterocycle from the side chain of the chromophore-forming Thr66 (*50*). The formation of a similar three ring chromophore featuring a 2-hydroxy-3-thiazoline ring is responsible for the orange fluorescence of the monomeric version of the reef coral FP Kusabira Orange (*51*).

Finally, oxidation of the amide nitrogen and Cα of the first amino acid of the chromogenic triad yields an acylimine bond that conjugates to the *p*-HBI system and causes the red-shifted fluorescence of proteins such as dsRed or eqFP611 (*16, 20, 55, 52-54*).

At present, the most red shifted emission maximum of naturally occurring FPs is found in eqFP611 from the sea anemone *Entacmaea quadricolor* (*16*). A further red shift of fluorescence could be achieved in engineered variants of red fluorescent proteins or non-fluorescent chromoproteins (*20*). In mPlum, the red shift is presumably induced by bringing the carbonyl oxygen of the amino acid preceding the first chromogenic residue into a coplanar arrangement with the chromophore (*55*). The red shift of RFP639 is likely caused by optimized π-stacking interactions of His197 and the phenyl group of the chromogenic tyrosine as a result of a trans-cis isomerisation of the chromophore (*24, 56*).

Great experimental opportunities arise from the diversity of fluorophores for multicolor labeling of proteins, cellular compartments or cells as well as for novel sensors based on fluorescence resonance energy transfer between FPs of different colors (*8, 39, 57, 66*). Currently, at least five differently colored FPs can be imaged in parallel (*8, 59*). Imaging of cells and tissues with RFPs is facilitated by the better penetration of cells and tissues by long wavelength light and reduced cellular

autofluorescence in the red emission range. These features make RFPs particularly interesting in the context of whole body imaging, for instance to monitor tumor progression in mouse models (*60*). The unstable variant AQ14 of the chromoprotein aeCP597 demonstrates that emission maxima as far to the red as 663 nm can be realized in FPs (*44*). However, further efforts are required to produce FPs in this emission range with bright and stable fluorescence for whole body imaging applications. At present, it remains unclear if the emission of FPs can be shifted still further to the infrared. Most recently, alternative marker proteins derived from bacterial phytochromes were introduced that have potential to fulfill the demand for live-cell compatible labels in the infrared range (*61*).

LIGHT-INDUCED ACTIVATION OF THE CHROMOPHORE

The imaging applications described in the previous section benefit from the autocatalytic formation of the chromophores in the presence of oxygen. Remarkably, the fluorescence properties of some FPs can be modified by irradiation with light of specific wavelengths (*18*). In GFP variants, irradiation with intense light around 400 nm results in transformation of the *p*-HBI chromophore from a nonfluorescent, neutral form to the fluorescent anionic state. The concomitant decarboxylation of Glu212 stabilizes the fluorescent chromophore and was exploited to generate a photoactivatable GFP (paGFP) (*62*). In another group of FPs, the *p*-HBI chromophore can be converted irreversibly from a green to a red fluorescent state by a photochemical modification of the peptide backbone. In EosFP, Kaede and several other anthozoan FPs and variants, irradiation with ~400 nm results in a cleavage of the peptide backbone between N_α and C_α of the first chromophore-forming residue histidine (*63-67*). Thereby, the conjugated π-electron system is extended in the imidazole sidechain of histidine. In a third group of FPs, cis–trans isomerisation of the chromophore is responsible for a reversible switching between bright and dark states of the chromophore (*32, 47, 68, 69*). Usually, the dark chromophore adopts a trans, noncoplanar conformation, whereas the bright state is associated with a cis, planar conformation (*32, 47*). Reversibly switchable chromophores are usually found in engineered green and red FPs (*70-73*), but also some natural GFP-like proteins feature switchable chromophores such a cerFP512 from a deep sea cerianthid (*74*). IrisFP combines two photoactivation processes in one FP: It can be photoconverted from a green to a red fluorescent form by irradiation with ~400 nm light but both, the green and the red chromophore can be reversibly switched off by irradiation with blue and green light, respectively (*32*). An overview of photoconvertible and photoswitchable proteins is given in Table 2.

Light-driven modulation of fluorescence properties opened up exciting opportunities for live cell imaging. Especially green to red photoconvertible proteins are useful for regional optical marking experiments because of the high optical contrast that is generated between the green- and the red-emitting state. Moreover, the wavelength of light applied for photoconversion is well separated from those wavelengths required for imaging the green and the red fluorophores (Table 2). Thus, the risk of unintentional photoactivation is greatly reduced. Imaging applications utilizing photoconvertible proteins include the tracking of fusion proteins within cells or subcellular compartments, tracking of single organelles such as mitochondria or cell fate mapping during embryonic development (Fig. 2) (*38, 82, 95*). Finally, FPs with photoconvertible chromophores play an important role in microscopy concepts that enable imaging beyond the diffraction barrier (*84-87*). Photo-activated localization microscopy (PALM) and related methods use targeted irradiation of photoactivatable probes to generate such a small amount of visible fluorophores in the sample that their diffraction-blurred images do not overlap (*88*). Subsequently, the precise localization of single fluorophores is determined within a few ten nanometers (as compared to the optical resolution of ~200 nm). After imaging, the emitting molecules are switched off and the cycle is repeated numerous times. Finally, a super-resolved image is assembled from all "pixels" generated during the experiment. Excellent results were obtained with labels such as the tandem dimer variant of EosFP (Fig. 2) (*79, 84*). Besides a large number of photons emitted by the fluorophore before photobleaching, a high optical contrast in the detection channel of the microscope, in which the individual, photoactivated FPs are measured, is important. However, photoconversion is an irreversible reaction and the activated red fluorophores need to be bleached after imaging of each frame. This might become a disadvantage if very small structures need to be visualized that contain less fluorophores than required for the construction of an image. In contrast to photoconvertible FPs, variants that can be reversibly switched on and off can be used in several imaging cyles. In the absence of photobleaching, the amount of pixels generated per fluorophore can be increased in dependence of the capacity of the fluorophore to undergo multiple switching cyles. Thereby, the amount of pixels required for imaging might be reached that could not be provided by photoconvertible FPs. Recently, techniques were developed, that enable live cell superresolution microscopy (*89*), so the generation of reversibly photoswitchable FPs in the red spectral range is highly desirable (*70, 71, 81*). FPs such as IrisFP that allow to control multiple phototransformations offer exciting perspectives for imaging applications including dynamic protein tracking with superresolution. Overall, great potential lies ahead for reversibly photoswitchable RFPs once limitations such as low brightness, oligomerization and fast photobleaching are overcome.

OLIGOMERIZATION AND AGGREGATION

In solution, avGFP is monomeric at concentrations below 1 mg/ml (Fig. 3) (*2*). In contrast, the red fluorescent protein dsRed from *Discosoma* sp. (*90*) forms tetramers. Subsequent analyzes of a variety of native and recombinant GFP-like

Table 2
FPs with activatable fluorescence

FP variant	Oligomerization degree (no. of protomers)	Type of fluorescence activation	Wavelengths (nm) required for fluorescence activation	Excitation maximum (nm)	Emission maximum (nm)	Molar extinction coefficient	Quantum yield	Relative brightness[a] (% of EGFP)
PA-GFP (*62*)	1	Off–On	488	504	517	17,400	0.79	43
PS-CFP (*75*)	1	Cyan–Green Conversion	405	402/490	468/511	34,000/27,000	0.16/0.19	17/16
Kaede (*64*)	4	Green–Red Conversion	~400	508/572	518/580	98,800/60,400	0.88/0.33	273/63
KikGR (*76*)	4	Green–Red Conversion	~400	507/583	517/593	53,700/35,100	0.70/0.65	118/72
EosFP (*66*)	4	Green–Red Conversion	~400	506/571	516/581	72,000/41,000	0.70/0.62	159/80
Dendra2 (*77*)	1	Green–Red Conversion	~400	490/553	507/573	45,000/35,000	0.50/0.55	71/61
mKikGR (*78*)	1	Green–Red Conversion	~400	505/580	515/591	49,000/28,000	0.69/0.63	106/56
tdEosFP (*79*)	1	Green–Red Conversion	~400	506/569	516/581	84,000/33,000	0.66/0.60	174/62
mEosFP (*66*)	1	Green–Red Conversion	~400	505/569	516/581	67,200/37,000	0.64/0.62	135/72
mEosFP2 (*80*)	1[b]	Green–Red Conversion	~400	506/573	519/584	56,000/46,000	0.84/0.66	148/96
Dronpa (*73*)	1	Reversible On/Off switching	~400/~488	503	518	95,000	0.85	254
rsFastLime (*72*)	1	Reversible On/Off switching	~400/~488	496	518	39000	0.77	94
rsCherry (*81*)	1	Reversible On/Off switching	~450/~550	572	610	80,000[c]	0.005[c]	5
rsCherryRev (*81*)	1	Reversible On/Off switching	~450/~550	572	608	84,000[c]	0.02[c]	1.3
PAmCherry1 (*70*)	1	Reversible On/Off switching	390–440/ 570	570	596	18,000	0.46	26
IrisFP (*32*)	4	Green–Red Conversion, Reversible On/Off switching	405 (conversion) ~400/~488 (green) ~440/532 (red)	488/551	516/580	52,200/35,400	0.43/0.47	71/52

[a]Determined for purified proteins.
[b]Dimerization tendency (*80*).
[c]Data from reference (*70*).

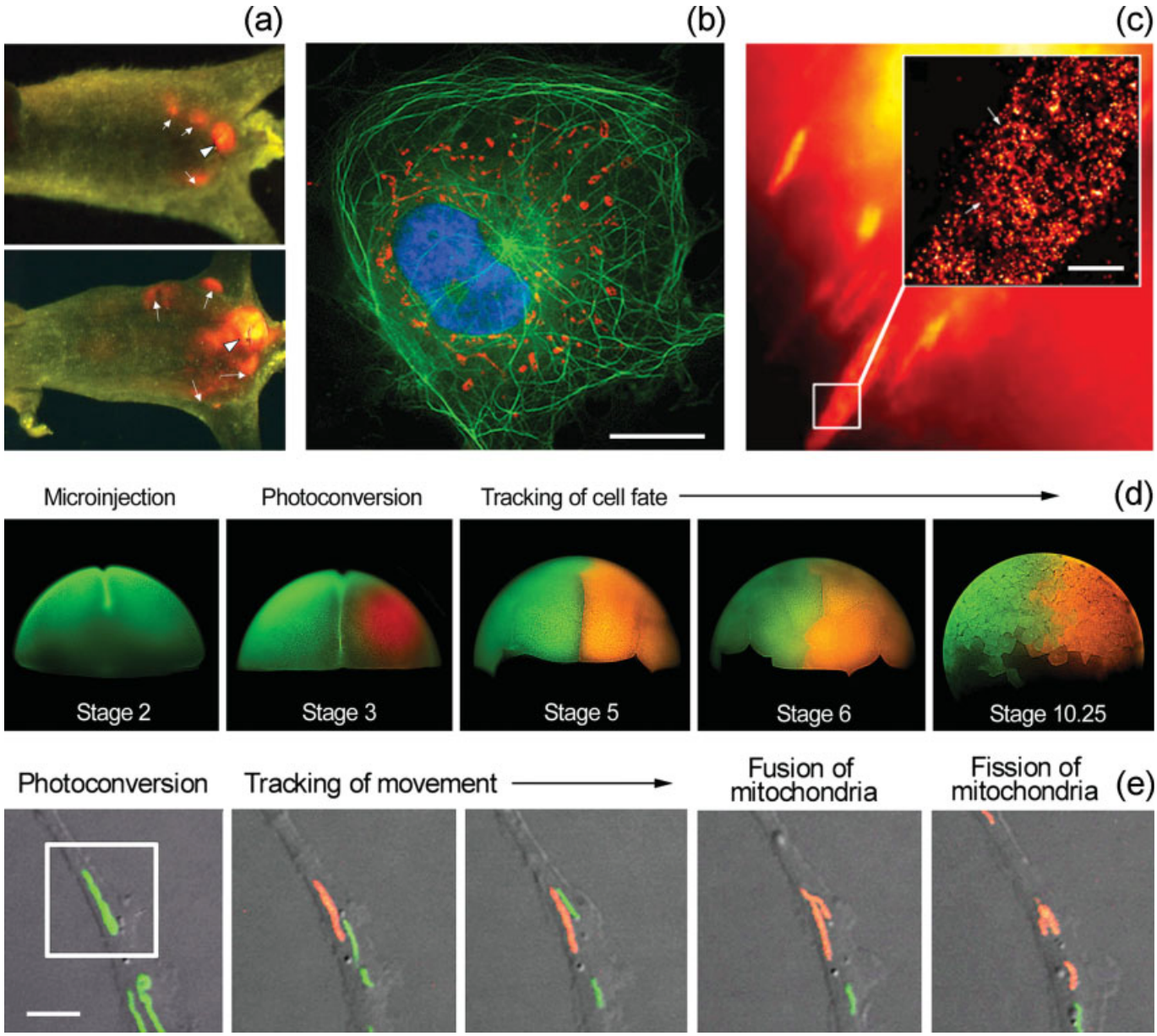

Figure 2. Applications of GFP-like proteins. Whole-body imaging of tumor progression in nude mice using DsRed-2 (a), showing the same animal two (upper panel) and four (lower panel) weeks after implantation of the tumor. Arrowhead: primary tumor; arrows: metastases. Multicolor imaging in HeLa cells (b). Green: EGFP-labeled tubulin-associated protein; red: mitochondrial RFP611, blue: nuclear DAPI stain, bar: 10 μm. Application of photoconvertible td-EosFP in super-resolution imaging (c). The widefield image shows td-EosFP-vinculin localization in focal adhesions. Inset: PALM image of a focal adhesion spot imaged with 20–30 nm resolution, arrows indicate a network-like structure, bar: 0.2 μm. Cell tracking during early embryonic development of *Xenopus laevis* (d). Purified EosFP was microinjected at stage 2. The fate of cells descending from a single blastomer can be followed by the red fluorescence after regional optical marking at stage 3. Labeling and tracking of organelles (e). Mitochondria were labeled green with td-EosFP. A single mitochondrion was photoconverted from green to red by irradiation with 405 nm light in the region indicated by the white rectangle. The fate of the labeled mitochondrion can be tracked by the red fluorescence, bar: 1 μm. (a, d) adapted from refs. (*60*) and (*82*). Copyright 2005/2009 Wiley-VCH Verlag GmbH& Co. KGaA, Weinheim, reproduced with permission. (b) reprinted from ref. (*24*). Copyright 2009, with permission from Elsevier. (c, e) Images courtesy of Michael W. Davidson, Florida State University.

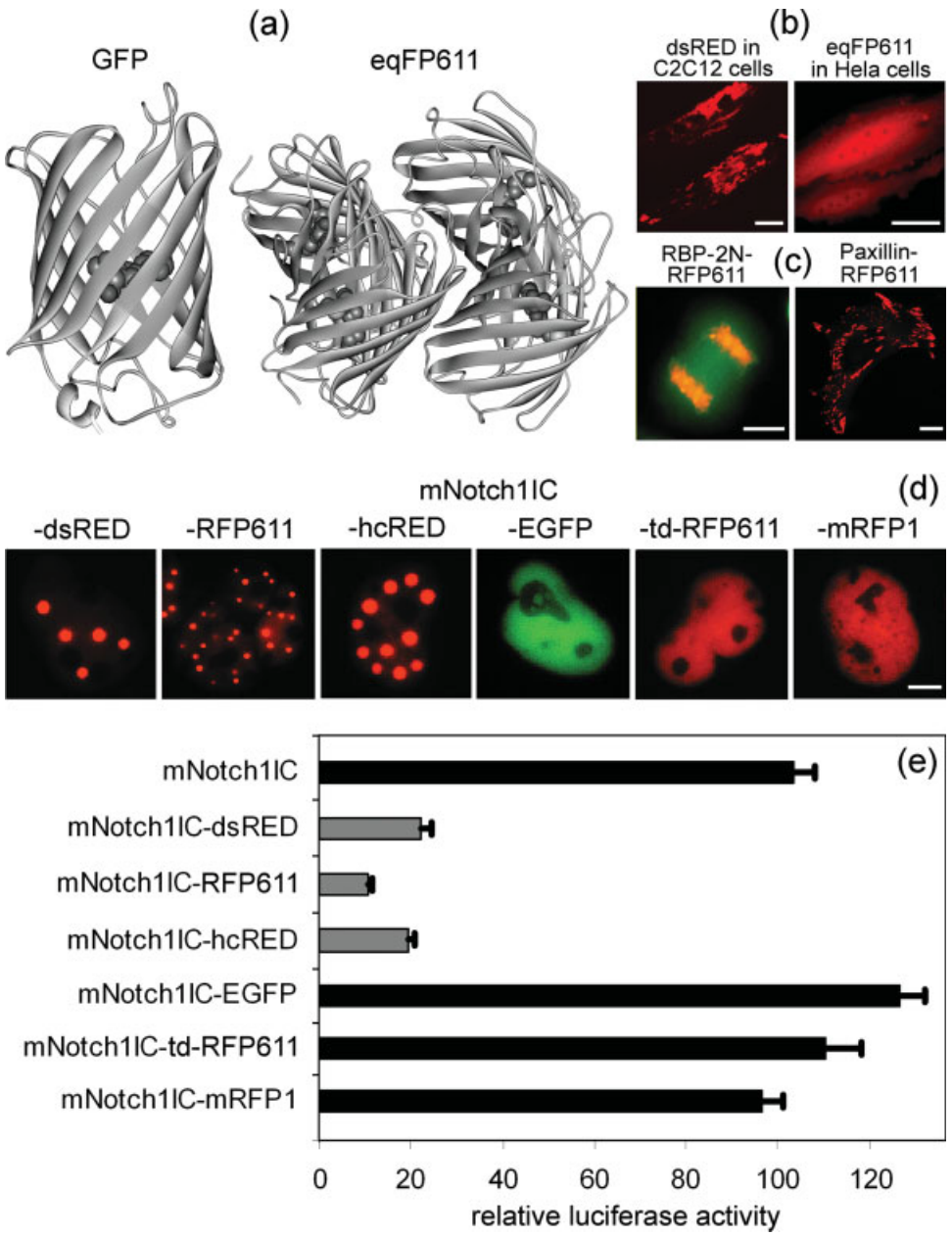

Figure 3. FP structures and implications for marker applications. Ribbon diagrams of monomeric GFP and tetrameric eqFP611 (a). Chromophores are shown as van der Waals spheres. Differences in aggregation tendency among unmodified RFPs from anthozoans (b). DsRed aggregates (left panel), uniform distribution of eqFP611 (right panel), bars: 10 μm. Correct cellular localization of proteins fused to tetrameric RFP611 (c). Chromatin-association of RBP-2N-RFP611 in a dividing HEK293 cell, EGFP highlights the cytoplasm (left panel), paxillin-RFP611 in focal adhesion of a Hela cell (right panel), bars: 5 μm. mNotch1IC, the activated form of the Notch receptor, shows a vesicle-like localization in the nuclei of transfected HEK293 cells in fusion with tetrameric (DsRed, eqFP611) and dimeric (HcRed) FPs, but an essentially uniform distribution in fusion with monomeric (EGFP, mRFP1) or pseudo-monomeric (td-RFP611) FPs, bar: 2.5 μm (d). The transactivation capacity of mNotch1IC determined by a luciferase assay (*66*)) is reduced in fusion with multimeric FPs (e). Panels (c) are reprinted from ref (*24*). Copyright 2009, with permission from Elsevier.

proteins from anthozoans showed that all of them were tetrameric (Fig. 3) (*20*). However, a small number of dimeric FPs were also found, such as the cyan FP MiCy from a scleractinian coral or the orange-red FP eqFP578 from the sea anemone *Entacmaea quadricolor* (*91, 38*). Another exception is a monomeric GFP isolated from the copepod *Pontellina plumata* (*17*). All X-ray structures of fluorescent and non-fluorescent GFP-like proteins from anthozoan species examined so far showed a tet-

rameric arrangement of the proteins in the crystal (Fig. 3) (*53, 92-94*).

If GFP is expressed as a fusion construct with another protein in cells, the concentrations can be usually considered to be in the range at which the protein molecules exist mostly as monomers. However, when a specific cellular localization creates a high local concentration, dimerization of the fusion proteins can be induced via the fluorescent tag, which might result in a loss of function or mislocalization of the protein. By replacing hydrophobic amino acid in the C-terminal region of EGFP, CFP, and YFP, in particular by the exchange Ala206Lys, truly monomeric derivatives were created (*10*).

The monomerization of anthozoan FPs often proved to be a more laborious task: In the red fluorescent proteins mRuby and mRFP1, 28 and 33 amino acids, respectively, had to be exchanged by various mutagenesis techniques that act in concert to recover functional expression of the monomeric forms (*39, 95*). Nevertheless, recent years yielded a considerable toolbox of monomeric FPs for protein labeling (Table 1).

It is important to distinguish between the defined oligomerization among anthozoan FPs that results in dimeric or tetrameric associations and the aggregation tendency that was observed, for instance, for dsRed and other anthozoan FPs (*46*). Aggregation results in the formation of clusters of precipitated proteins that become microscopically visible upon recombinant expression in a range of mammalian cells. In some cases, the apparent aggregation was due to the accumulation of the marker protein in lysosomes (*96*). The tendency to form aggregates varies among different natural RFPs, ranging from pronounced in dsRed to virtually absent in eqFP611 (*16, 46*). For several fusion proteins, the aggregation tendency of the marker prevented the correct localization of the fusion protein (*97*). Moreover, the vitality of cells can be adversely affected by formation of marker protein aggregates (*40, 98*). In contrast, formation of soluble dimeric or tetrameric associations does not automatically generate adverse effects as long as no unspecific aggregates are formed. Applications, in which the oligomerization degree is irrelevant, include labeling of whole cells for cell fate mapping or cell tracking, the labeling of cellular organelles, gene expression studies including expression-based sensor applications. In such cases, the experiment can benefit from the often excellent brightness and thermodynamic stability of multimeric marker proteins. It is also worth mentioning that tetramerization does not necessarily interfere with the correct localization of fusion proteins (Fig. 2) (*24*). However, in many cases the fluorescent marker protein needs to be monomeric for correct localization of the fusion partner as exemplified for α-tubulin. Only if the fused FPs are strictly monomeric, the formation of tubulin fibers can be observed (*25, 38*). Another example is the localization of the intracellular domain of the mouse Notch1 receptor (mNotch1IC). Compared with the nuclear localization of some monomeric or pseudo-monomeric tandem dimers, the oligomerization of the fused marker protein is correlated with a significantly different localization (Fig. 3). The alternative localization also results in altered functionality of mNotch1IC as deduced from its reduced transactivation capacity in reporter gene assays (Fig. 3).

THE QUESTION OF BRIGHTNESS

The key property of FPs is their brightness as it directly influences their usefulness in imaging. Brightness is the product of the capabilities of the chromophores to absorb light (described by the molar extinction coefficient) and to re-emit photons (described by the quantum yield of fluorescence). Consequently, the higher the extinction coefficient and quantum yield are, the brighter is the fluorescence of the marker protein. In practice, especially the determination of the extinction coefficient of RFPs is not trivial. Often, the bulk of recombinantly expressed proteins can contain unfolded molecules or proteins with immature green chromophores or chromophores in dark states. Since the concentration of the proteins is usually determined by the absorption of the aromatic residues at 280 nm, these molecules contribute to the overall concentration but not to the absorption in the expected range. Consequently, the extinction coefficient of the functional red chromophores will be underestimated. Methods such as the alkaline denaturation method or the dynamic difference method have been developed to take only functional chromophores into account and may yield more precise values for the individual chromophore types (*45, 39*).

Furthermore, the physical property brightness associated with a certain FP only partially describes how bright the FP is in an imaging application. What counts is not only the brightness of the individual fluorophore, but also the total amount of functional molecules expressed. This quantity depends on a multitude of factors: How well is the construct transcribed? How well is the construct translated? How many of the expressed proteins develop functional chromophores? How fast is the turnover of the functional molecules? How fast does photobleaching occur? These issues are further complicated by additional variations for different cell types. The example of mEosFP demonstrates how the expression temperature can affect the cellular brightness. The protein can be employed successfully as a bright cellular marker in a range of organisms, including plants, drosophila or zebrafish, but no fluorescence is observed in mammalian cells cultured at 37°C (*66, 99, 100*). Despite its excellent molecular brightness, mEosFP does not fold correctly at temperatures above 30°C. It is interesting to mention in this context that the temperature dependence of folding of FPs does not necessarily track the temperature range the pigmented animals experience in their natural habitats: eqFP611 from a tropical sea anemone living in waters with temperatures between 24 and 28°C does not become functional at temperatures >30°C (*16*). In contrast, cerFP505 folds properly at 37°C despite originating from a deep sea cerianthid adapted to a life at temperatures between 4 and 7°C (*74*).

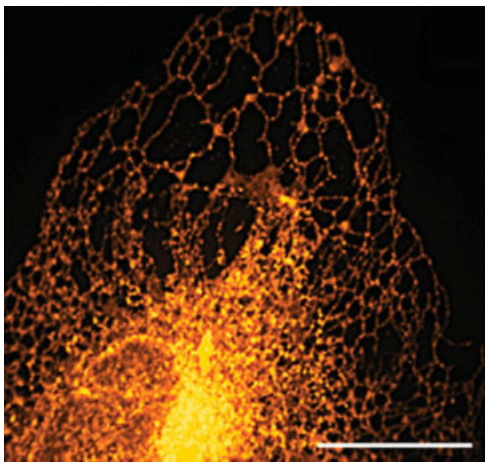

Figure 4. Spinning disc confocal microscopy image shows the endoplasmic reticulum of a HeLa cell brightly stained with ER-mRuby-KDEL. The fluorescence intensity is encoded by false colors, bar: 2.5 μm. Image reprinted from ref. (*39*).

The importance of efficient translation was demonstrated during development of the monomeric RFP mRuby. Its cellular brightness could be increased by 5 – 8-fold by optimizing the codon usage for expression in mammalian cells (*39*). The localization in different cellular compartments can also affect the brightness of the labels. mRuby is 1.2-fold brighter than EGFP when compared on the level of purified proteins, but ~10-fold brighter when targeted to the endoplasmic reticulum (Fig. 4) (*39*). This effect is correlated with an exceptional resistance of mRuby towards pH extremes that might indicate a general stability of the particular variation of the β-can fold (*39*). Finally, the distance between excitation and emission maximum, the Stokes shift, is important for the detectability of the marker in devices depending on optical filter systems such microscopes or FACS machines: The larger the Stokes shift, the better is the separation of the excitation and emission light and consequently, the signal to noise ratio. Fluorescent proteins with extraordinarly large Stokes shifts can be found among red and far-red proteins (Table 1).

In summary, the search for the optimal marker protein for distinct applications should not only be guided by the molecular brightness of FPs, but also by comparative expression tests of several potentially suitable marker proteins.

MATURATION TIME

Chromophore maturation in FPs consists of two components, the folding of the protein molecule and the autocatalytic formation of the chromophore. In GFP, folding occurs with a $t_{0.5}$ of ~10 min. The chemical reactions (cylization, dehydration and oxidation) that yield the functional chromophore are considerably slower ($t_{0.5}$ = 22–86 min) (*5*). The maturation times of red fluorescent proteins from various anthozoans differ considerably. For eqFP611, most of the molecules have reached their fluorescent state within 12 h (*16*). In contrast, wildtype dsRed takes more than 4 days to develop its maximal red fluorescence (*90*). Protein engineering could greatly accelerate the maturation process of RFP derivatives, yielding variants that become fully functional with a t_{05} between 0.3 h and 3.0 h (Table 1). We note that these values were determined by different methods and might be not directly comparable. The maturation times of FPs were often deduced from experiments on purified proteins (*39*). However, if cells are transfected with DNA, a certain time is required until the DNA molecules migrate to the nucleus and are transcribed. This period can be shortened if the cells are injected with mRNA. Then, the above described factors influencing the concentration of functional fluorophores determine when a threshold for detection is reached.

Taken together, all these factors delay the time when the marker protein can be detected in living cells. After transfection with EGFP expression vectors, the first green fluorescent cells can be observed after ~6.5 h in a standard fluorescence microscope (*21*). The lag period between introduction of the genetic information and the detectability of the marker can hamper studies such as monitoring early embryonic development: After *Xenopus* embryos were microinjected with capped mRNA encoding EosFP at the four cell stage, it took ~6.5 h until sufficient amounts of the marker protein were present to allow photoconversion and cell fate mapping experiments (*82*). The "blind spot" during the first hours of development can be avoided if purified EosFP protein is injected to allow immediate optical marking.

At present, maturation times of engineered RFPs allow their application in most protein labeling experiments by using a standard overnight expression protocol. However, for experiments that require fast detection of the presence of the FPs, for instance certain gene expression studies, different FPs should be tested in the specific cellular context. Accelerated maturation is desirable for future generations of engineered marker proteins.

SIDE EFFECTS OF FPS IN MARKER APPLICATIONS

GFP and its natural color variants are used as markers in recombinant systems in the belief that they behave mostly neutral towards the physiology of the cell. This view is justified by the vast number of experiments in which FPs were applied without obvious side effects. Still, one has to consider the possibility that the experimental setup might affect the results.

Photoactivation and Light-Induced Cytotoxicity

The detection of FPs in living cells and tissues requires their excitation with a light or laser source, and photoactivation also uses light of specific wavelengths. Light, especially of short wavelengths, can induce phototoxic effects in cells (*101-103*). The action spectrum of phototoxicity shows a decrease towards longer wavelengths, which can be mainly explained by the reduced amount of potential photosensitzers that absorb longer

wavelength light. However, phototoxicity not only depends on the wavelength, but also on the total dose of incident light (*102*). In consequence, cytotoxic effects potentially accompanying the application of an FP relate to both, the wavelength and the intensity of the light required for imaging or photoconversion and photoswitching. In conventional wide field microscopy, this amount of photons depends on the number of functional FP chromophores present in the cell, the extinction coefficient of the chromophore at the targeted waveband and the quantum yields of the photophysical/photochemical reactions.

In summary, the application of FPs that can be excited, photoconverted or photoswitched with light of longer wavelengths potentially reduces the risk of cytotoxic effects, but only if they are equally bright and have comparably high photoactivation/photoconversion quantum yields than their short-wavelength counterparts. EosFP-labeled *Xenopus* embryos showed no obvious negative response to photoconversion procedure with violet-blue light and developed normally for at least 4 months (*82*). The lack of obvious phototoxic effects in irradiated *Xenopus* embryos is probably due to the fairly small amount of short wavelength light required for photoconversion. Photoconversion/photoswitching proceeds usually via the neutral chromophore that absorbs at shorter wavelengths as the anionic form (*32, 66*). Consequently, shifting of the ground state equilibrium towards the neutral form can increase the conversion/switching efficiency and allows to reduce the dose of irradiation required to achieve the desired effect (*104, 105*). However, the increase in conversion efficiency will come at the expense of brightness that is lowered along with the concentration of the anionic chromophore.

Some of the negative effects associated with the exposure of cells to UV and visible light can be circumvented by alternative microscopy methods such as two-photon microscopy, which uses infrared light for imaging and manipulation of the FPs (*76, 106-108*). More research is required to clarify to which extent photobleaching and triplet formation of the FP-chromophores mediate cytotoxic effects via the generation of reactive oxygen species (ROS). ROS production appears to be generally rather low in GFP and GFP-like proteins (*109, 110*) but differences in phototoxicity were observed among some engineered RPF variants (*40*).

FP-induced Cytotoxicity

Fusing a GFP or GFP-like protein to a protein of interest can impair the function of the latter, and expression of this construct can adversely affect cellular function (Fig. 3) (*97*). Already expression of the plain FP in a cell may induce cytotoxic effects (*40, 98*). Cytotoxicity of GFP could be enhanced by the fusion of a peptide that increases the aggregation tendency of the molecules (*111*). Optimized codon usage significantly reduced the cytotoxicity of EosFP in murine stem cells (Fig. 5), indicating that even rather unspecific effects of overexpression might account for cytotoxicity of some FPs. Finally, because the biological function of FPs is still unclear, a yet unknown biological activity exerted by FPs might affect the physiological response of the recombinant expression system.

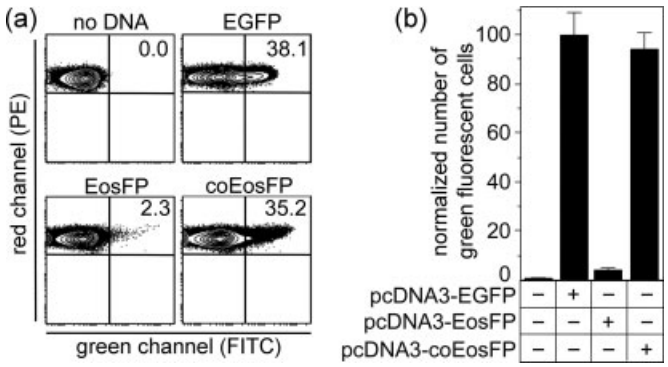

Figure 5. Effect of codon-usage on cytotoxicity in murine embryonic stem cells. ES cells expressing td-RFP from the ROSA26 locus (*112*) were transiently transfected with vector DNA for expression of EGFP, EosFP and the codon-optimized EosFP variant (coEosFP). (a) Representative FACS diagrams showing the amount of red and green fluorescent cells 48 hours after transfection. (b) Number of green fluorescent cells normalized to EGFP-expressing cells. The bar diagram shows the mean of three replicate experiments. Error bars indicate standard deviation.

Numerous reef corals accumulate FPs to impressive amounts of >10% of the total soluble protein content of their tissue with some of their genes being tightly regulated by the amount of incident blue light (*63, 113*). This response suggests a role of FPs in the photobiology of the animals and/or their symbiotic algae, but the mechanism how they might fulfill, for instance, a photoprotective function is still subject of debate (*113*). However, the presence of remotely related anthozoan taxa with intense GFP-coloration in low light habitats including the deep sea may argue against a general photoprotective role of these pigments (*21, 74*). Recently, a nuclear export signal and a peroxisomal targeting signal were identified in wildtype forms of asFP499 and eqFP611 (*39, 114*). These signals may also hint at different specific functions of the proteins in the organisms they were isolated from. To understand the potential influence of the markers on the experimental outcome, further research on the biological function of the pigments is required.

CONCLUSION

The impact of the fluorescent protein technology was greatly enhanced by the introduction of GFP-like proteins from various marine invertebrates. Cellular imaging applications involving multicolor labeling, whole body imaging, dynamic tracking and superresolution microscopy benefit enormously from the novel FPs, especially from red fluorescent proteins and photoconvertible/photoswitchable GFP-like proteins and their engineered var-

iants. At present, a large toolbox of fluorescent markers is available, but none of the FPs is equally well suited for all imaging purposes. Application relevant properties such as fluorescence brightness depend not only the structure of the molecule but also on the cellular environment in which the marker protein is expressed. Hence, comparative tests are recommended to find the ideal marker for an experiment. Further engineering efforts should be dedicated to provide FPs with accelerated maturation time, increased photostability, and further red-shifted emission whereas emerging superresolution microscopy techniques call for optimized photoswitchable RFPs.

ACKNOWLEDGEMENTS

This work was supported by the Deutsche Forschungsgemeinschaft (DFG) and the State of Baden-Württemberg through the Center for Functional Nanostructures (CFN), by DFG grants Wi1990/2-1 to J.W., Ni 291/9 to GUN, SFB 497 to FO and GUN, SFB 518 to FO, by the Fonds der Chemischen Industrie to GUN, by the Landestiftung Baden-Württemberg (Elite Postdoc Program to JW and by the University of Southampton (NOC/SOM interface fund to JW).

REFERENCES

1. Shimomura, O., Johnson, F. H., and Saiga, Y. (1962) Extraction, purification and properties of aequorin, a bioluminescent protein from the luminous hydromedusan, *Aequorea*. *J. Cell. Comp. Physiol.* **59**, 223–239.
2. Ward, W. W. Chalfie, M., and Kain, S. R., eds. (2005) *Biochemical and physical properties of green fluorescent protein. Green fluorescent protein: properties, applications and protocols*, 2nd edn. pp. 39–65, Wiley, Hoboken, USA.
3. Prasher, D. C., Eckenrode, V. K., Ward, W. W., Prendergast, F. G., and Cormier, M. J. (1992) Primary structure of the *Aequorea victoria* green-fluorescent protein. *Gene* **111**, 229–233.
4. Chalfie, M., Tu, Y., Euskirchen, G., Ward, W. W., and Prasher, D. C. (1994) Green fluorescent protein as a marker for gene expression. *Science* **263**, 802–805.
5. Tsien, R. Y. (1998) The green fluorescent protein. *Annu. Rev. Biochem.* **67**, 509–544.
6. Griesbeck, O. (2004) Fluorescent proteins as sensors for cellular functions. *Curr. Opin. Neurobiol.* **14**, 636–641.
7. Chalfie, M. and Kain, S. R. (2005) *Green fluorescent protein: properties, applications and protocols*. Wiley, Hoboken, USA.
8. Shaner, N. C., Patterson, G. H., and Davidson, M. W. (2007) Advances in fluorescent protein technology. *J. Cell. Sci.* **120**, 4247–4260.
9. Pedelacq, J. D., Cabantous, S., Tran, T., Terwilliger, T. C., and Waldo, G. S. (2006) Engineering and characterization of a superfolder green fluorescent protein (vol 24, pg 79, 2005). *Nat. Biotechnol.* **24**, 1170–1170.
10. Zacharias, D. A., Violin, J. D., Newton, A. C., and Tsien, R. Y. (2002) Partitioning of lipid-modified monomeric GFPs into membrane microdomains of live cells. *Science* **296**, 913–916.
11. Nienhaus, G. U. (2008) The green fluorescent protein: a key tool to study chemical processes in living cells. *Angew. Chem. Int. Ed.* **47**, 8992–8994.
12. Mishin, A. S., Subach, F. V., Yampolsky, I. V., King, W., Lukyanov, K. A., and Verkhusha, V. V. (2008) The first mutant of the *Aequorea victoria* green fluorescent protein that forms a red chromophore. *Biochemistry* **47**, 4666–4673.
13. Wiedenmann, J. (1997) The application of an orange fluorescent protein and further colored proteins and the corresponding genes from the species group *Anemonia* sp. (*sulcata*) Pennant, (Cnidaria, Anthozoa, Actinaria) in gene technology and molecular biology. Deutsches Patent und Markenamt. Patent DE 19718640.
14. Matz, M. V., Fradkov, A. F., Labas, Y. A., Savitsky, A. P., Zaraisky, A. G., Markelov, M. L., and Lukyanov, S. A. (1999) Fluorescent proteins from nonbioluminescent Anthozoa species. *Nat. Biotechnol.* **17**, 969–973.
15. Fradkov, A. F., Chen, Y., Ding, L., Barsova, E. V., Matz, M. V., and Lukyanov, S. A. (2000) Novel fluorescent protein from Discosoma coral and its mutants possesses a unique far-red fluorescence. *FEBS. Lett.* **479**, 127–130.
16. Wiedenmann, J., Schenk, A., Rocker, C., Girod, A., Spindler, K. D., and Nienhaus, G. U. (2002) A far-red fluorescent protein with fast maturation and reduced oligomerization tendency from *Entacmaea quadricolor* (Anthozoa, Actinaria). *Proc. Natl. Acad. Sci. USA* **99**, 11646–11651.
17. Shagin, D. A., Barsova, E. V., Yanushevich, Y. G., Fradkov, A. F., Lukyanov, K. A., Labas, Y. A., Semenova, T. N., Ugalde, J. A., Meyers, A., Nunez, J. M., Widder, E. A., Lukyanov, S. A., and Matz, M. V. (2004) GFP-like proteins as ubiquitous metazoan superfamily: evolution of functional features and structural complexity. *Mol. Biol. Evol.* **21**, 841–850.
18. Wiedenmann, J. and Nienhaus, G. U. (2006) Live-cell imaging with EosFP and other photoactivatable marker proteins of the GFP family. *Exp. Rev. Prot.* **3**, 361–374.
19. Alieva, N. O., Konzen, K. A., Field, S. F., Meleshkevitch, E. A., Hunt, M. E., Beltran-Ramirez, V., Miller, D. J., Wiedenmann, J., Salih, A., and Matz, M. V. (2008) Diversity and evolution of coral fluorescent proteins. *PLoS ONE* **3**, e2680.
20. Nienhaus, G. U. and Wiedenmann, J. (2009) Structure, dynamics and optical properties of fluorescent proteins: perspectives for marker development. *Chemphyschem* **10**, 1369–1379.
21. Wiedenmann, J., Ivanchenko, S., Oswald, F., and Nienhaus, G. U. (2004) Identification of GFP-like proteins in nonbioluminescent, azooxanthellate anthozoa opens new perspectives for bioprospecting. *Mar. Biotechnol.* **6**, 270–277.
22. Deheyn, D. D., Kubokawa, K., Mccarthy, J. K., Murakami, A., Porrachia, M., Rouse, G. W., and Holland, N. D. (2007) Endogenous green fluorescent protein (GFP) in amphioxus. *Biol. Bull.* **213**, 95–100.
23. Ugalde, J. A., Chang, B. S., and Matz, M. V. (2004) Evolution of coral pigments recreated. *Science* **305**, 1433.
24. Kredel, S., Nienhaus, K., Oswald, F., Wolff, M., Ivanchenko, S., Cymer, F., Jeromin, A., Michel, F. J., Spindler, K. D., Heilker, R., Nienhaus, G. U., and Wiedenmann, J. (2008) Optimized and far-red-emitting variants of fluorescent protein eqFP611. *Chem. Biol.* **15**, 224–233.
25. Shaner, N. C., Campbell, R. E., Steinbach, P. A., Giepmans, B. N., Palmer, A. E., and Tsien, R. Y. (2004) Improved monomeric red, orange and yellow fluorescent proteins derived from *Discosoma* sp. red fluorescent protein. *Nat. Biotechnol.* **22**, 1567–1572.
26. Wang, L., Jackson, W. C., Steinbach, P. A., and Tsien, R. Y. (2004) Evolution of new nonantibody proteins via iterative somatic hypermutation. *Proc. Natl. Acad. Sci. USA* **101**, 16745–16749.
27. Shcherbo, D., Merzlyak, E. M., Chepurnykh, T. V., Fradkov, A. F., Ermakova, G. V., Solovieva, E. A., Lukyanov, K. A., Bogdanova, E. A., Zaraisky, A. G., Lukyanov, S., and Chudakov, D. M. (2007) Bright far-red fluorescent protein for whole-body imaging. *Nat. Methods* **4**, 741–746.
28. Wiedenmann, J., Elke, C., Spindler, K. D., and Funke, W. (2000) Cracks in the beta-can: fluorescent proteins from *Anemonia sulcata* (Anthozoa, Actinaria). *Proc. Natl. Acad. Sci. USA* **97**, 14091–14096.
29. Nienhaus, K., Renzi, F., Vallone, B., Wiedenmann, J., and Nienhaus, G. U. (2006) Chromophore-protein interactions in the anthozoan green fluorescent protein asFP499. *Biophys. J.* **91**, 4210–4220.

30. Ai, H.-W., Olenych, S. G., Wong, P., Davidson, M. W., and Campbell, R. E. (2008) Hue-shifted monomeric variants of Clavularia cyan fluorescent protein: identification of the molecular determinants of color and applications in fluorescence imaging. *BMC. Biol.* **6**, 1–13.
31. Henderson, J. N. and Remington, S. J. (2005) Crystal structures and mutational analysis of amFP486, a cyan fluorescent protein from Anemonia majano. *Proc. Natl. Acad. Sci. USA* **102**, 12712–12717.
32. Adam, V., Lelimousin, M., Boehme, S., Desfonds, G., Nienhaus, K., Field, M. J., Wiedenmann, J., Mcsweeney, S., Nienhaus, G. U., and Bourgeois, D. (2008) Structural characterization of IrisFP, an optical highlighter undergoing multiple photo-induced transformations. *Proc. Natl. Acad. Sci. USA* **105**, 18343–18348.
33. Remington, S. J., Wachter, R. M., Yarbrough, D. K., Branchaud, B., Anderson, D. C., Kallio, K., and Lukyanov, K. A. (2005) zFP538, a yellow-fluorescent protein from Zoanthus, contains a novel three-ring chromophore. *Biochemistry* **44**, 202–212.
34. Wachter, R. M., Elsliger, M. A., Kallio, K., Hanson, G. T., and Remington, S. J. (1998) Structural basis of spectral shifts in the yellow-emission variants of green fluorescent protein. *Structure* **6**, 1267–1277.
35. Patterson, G. H., Knobel, S. M., Sharif, W. D., Kain, S. R., and Piston, D. W. (1997) Use of the green fluorescent protein and its mutants in quantitative fluorescence microscopy. *Biophys. J.* **73**, 2782–2790.
36. Sakaue-Sawano, A., Kurokawa, H., Morimura, T., Hanyu, A., Hama, H., Osawa, H., Kashiwagi, S., Fukami, K., Miyata, T., Miyoshi, H., Imamura, T., Ogawa, M., Masai, H., and Miyawaki, A. (2008) Visualizing spatiotemporal dynamics of multicellular cell-cycle progression. *Cell* **132**, 487–498.
37. Shaner, N. C., Lin, M. Z., Mckeown, M. R., Steinbach, P. A., Hazelwood, K. L., Davidson, M. W., and Tsien, R. Y. (2008) Improving the photostability of bright monomeric orange and red fluorescent proteins. *Nat. Methods* **5**, 545–551.
38. Merzlyak, E. M., Goedhart, J., Shcherbo, D., Bulina, M. E., Shcheglov, A. S., Fradkov, A. F., Gaintzeva, A., Lukyanov, K. A., Lukyanov, S., Gadella, T. W., and Chudakov, D. M. (2007) Bright monomeric red fluorescent protein with an extended fluorescence lifetime. *Nat. Methods* **4**, 555–557.
39. Kredel, S., Oswald, F., Nienhaus, K., Deuschle, K., Roecker, C., Wolff, M., Heilker, R., Nienhaus, G. U., and Wiedenmann, J. (2009) mRuby, a bright monomeric red fluorescent protein for labeling of subcellular structures. *PLoS ONE* **4**, e4391.
40. Strack, R. L., Strongin, D. E., Bhattacharyya, D., Tao, W., Berman, A., Broxmeyer, H. E., Keenan, R. J., and Glick, B. S. (2008) A noncytotoxic DsRed variant for whole-cell labeling. *Nat. Methods* **5**, 955–957.
41. Kogure, T., Karasawa, S., Araki, T., Saito, K., Kinjo, M., and Miyawaki, A. (2006) A fluorescent variant of a protein from the stony coral Montipora facilitates dual-color single-laser fluorescence cross-correlation spectroscopy. *Nat. Biotechnol.* **24**, 577–581.
42. Shcherbo, D., Murphy, C. S., Ermakova, G. V., Solovieva, E. A., Chepurnykh, T. V., Shcheglov, A. S., Verkhusha, V. V., Pletnev, V. Z., Hazelwood, K. L., Roche, P. M., Lukyanov, S., Zaraisky, A. G., Davidson, M. W., and Chudakov, D. M. (2009) Far-red fluorescent tags for protein imaging in living tissues. *Biochem. J.* **418**, 567–574.
43. Gurskaya, N. G., Fradkov, A. F., Terskikh, A., Matz, M. V., Labas, Y. A., Martynov, V. I., Yanushevich, Y. G., Lukyanov, K. A., and Lukyanov, S. A. (2001) GFP-like chromoproteins as a source of far-red fluorescent proteins. *FEBS. Lett.* **507**, 16–20.
44. Shkrob, M. A., Yanushevich, Y. G., Chudakov, D. M., Gurskaya, N. G., Labas, Y. A., Poponov, S. Y., Mudrik, N. N., Lukyanov, S., and Lukyanov, K. A. (2005) Far-red fluorescent proteins evolved from a blue chromoprotein from *Actinia equina*. *Biochem. J.* **392**, 649–654.
45. Gross, L. A., Baird, G. S., Hoffman, R. C., Baldridge, K. K., and Tsien, R. Y. (2000) The structure of the chromophore within DsRed, a red fluorescent protein from coral. *Proc. Natl. Acad. Sci. USA* **97**, 11990–11995.
46. Yanushevich, Y. G., Staroverov, D. B., Savitsky, A. P., Fradkov, A. F., Gurskaya, N. G., Bulina, M. E., Lukyanov, K. A., and Lukyanov, S. A. (2002) A strategy for the generation of nonaggregating mutants of Anthozoa fluorescent proteins. *FEBS. Lett.* **511**, 11–14.
47. Andresen, M., Wahl, M. C., Stiel, A. C., Grater, F., Schafer, L. V., Trowitzsch, S., Weber, G., Eggeling, C., Grubmuller, H., Hell, S. W., and Jakobs, S. (2005) Structure and mechanism of the reversible photoswitch of a fluorescent protein. *Proc. Natl. Acad. Sci. USA* **102**, 13070–13074.
48. Quillin, M. L., Anstrom, D. M., Shu, X., O'leary, S., Kallio, K., Chudakov, D. M., and Remington, S. J. (2005) Kindling fluorescent protein from Anemonia sulcata: dark-state structure at 1.38 A resolution. *Biochemistry* **44**, 5774–5787.
49. Wilmann, P. G., Petersen, J., Devenish, R. J., Prescott, M., and Rossjohn, J. (2005) Variations on the GFP chromophore. *J. Biol. Chem.* **280**, 2401–2404.
50. Shu, X., Shaner, N. C., Yarbrough, C. A., Tsien, R. Y., and Remington, S. J. (2006) Novel chromophores and buried charges control color in mFruits. *Biochemistry* **45**, 9639–9647.
51. Kikuchi, A., Fukumura, E., Karasawa, S., Mizuno, H., Miyawaki, A., and Shiro, Y. (2008) Structural characterization of a thiazoline-containing chromophore in an orange fluorescent protein, monomeric Kusabira orange. *Biochemistry* **47**, 11573–11580.
52. Wiedenmann, J., Vallone, B., Renzi, F., Nienhaus, K., Ivanchenko, S., Rocker, C., and Nienhaus, G. U. (2005) Red fluorescent protein eqFP611 and its genetically engineered dimeric variants. *J. Biomed. Opt.* **10**, 14003.
53. Yarbrough, D., Wachter, R. M., Kallio, K., Matz, M. V., and Remington, S. J. (2001) Refined crystal structure of DsRed, a red fluorescent protein from coral, at 2.0-A resolution. *Proc. Natl. Acad. Sci. USA* **98**, 462–467.
54. Petersen, J., Wilmann, P. G., Beddoe, T., Oakley, A. J., Devenish, R. J., Prescott, M., and Rossjohn, J. (2003) The 2.0-angstrom crystal structure of eqFP611, a far red fluorescent protein from the sea anemone *Entacmaea quadricolor*. *J. Biol. Chem.* **278**, 44626–44631.
55. Abbyad, P., Childs, W., Shi, X. H., and Boxer, S. G. (2007) Dynamic stokes shift in green fluorescent protein variants. *Proc. Natl. Acad. Sci. USA* **104**, 20189–20194.
56. Loos, D. C., Habuchi, S., Flors, C., Hotta, J., Wiedenmann, J., Nienhaus, G. U., and Hofkens, J. (2006) Photoconversion in the red fluorescent protein from the sea anemone Entacmaea quadricolor: is cis-trans isomerization involved? *J. Am. Chem. Soc.* **128**, 6270–6271.
57. Goedhart, J., Vermeer, J. E., Adjobo-Hermans, M. J., Van Weeren, L., and Gadella, T. W. (2007) Sensitive detection of p65 homodimers using red-shifted and fluorescent protein-based FRET couples. *PLoS ONE* **2**, e1011.
58. Ai, H. W., Hazelwood, K. L., Davidson, M. W., and Campbell, R. E. (2008) Fluorescent protein FRET pairs for ratiometric imaging of dual biosensors. *Nat. Methods* **5**, 401–403.
59. Livet, J., Weissman, T. A., Kang, H., Draft, R. W., Lu, J., Bennis, R. A., Sanes, J. R., and Lichtman, J. W. (2007) Transgenic strategies for combinatorial expression of fluorescent proteins in the nervous system. *Nature* **450**, 56–62.
60. Yang, M., Jiang, P., Yamamoto, N., Li, L., Geller, J., Moossa, A. R., and Hoffman, R. M. (2005) Real-time whole-body imaging of an orthotopic metastatic prostate cancer model expressing red fluorescent protein. *Prostate* **62**, 374–379.
61. Shu, X. K., Royant, A., Lin, M. Z., Aguilera, T. A., Lev-Ram, V., Steinbach, P. A., and Tsien, R. Y. (2009) Mammalian expression of infrared fluorescent proteins engineered from a bacterial phytochrome. *Science* **324**, 804–807.
62. Patterson, G. H. and Lippincott-Schwartz, J. (2002) A photoactivatable GFP for selective photolabeling of proteins and cells. *Science* **297**, 1873–1877.

63. Oswald, F., Schmitt, F., Leutenegger, A., Ivanchenko, S., D'angelo, C., Salih, A., Maslakova, S., Bulina, M., Schirmbeck, R., Nienhaus, G. U., Matz, M. V., and Wiedenmann, J. (2007) Contributions of host and symbiont pigments to the coloration of reef corals. *FEBS. J.* **274**, 1102–1109.
64. Ando, R., Hama, H., Yamamoto-Hino, M., Mizuno, H., and Miyawaki, A. (2002) An optical marker based on the UV-induced green-to-red photoconversion of a fluorescent protein. *Proc. Natl. Acad. Sci. USA* **99**, 12651–12656.
65. Mizuno, H., Mal, T. K., Tong, K. I., Ando, R., Furuta, T., Ikura, M., and Miyawaki, A. (2003) Photo-induced peptide cleavage in the green-to-red conversion of a fluorescent protein. *Mol. Cell.* **12**, 1051–1058.
66. Wiedenmann, J., Ivanchenko, S., Oswald, F., Schmitt, F., Rocker, C., Salih, A., Spindler, K. D., and Nienhaus, G. U. (2004) EosFP, a fluorescent marker protein with UV-inducible green-to-red fluorescence conversion. *Proc. Natl. Acad. Sci. USA* **101**, 15905–15910.
67. Nienhaus, K., Nienhaus, G. U., Wiedenmann, J., and Nar, H. (2005) Structural basis for photo-induced protein cleavage and green-to-red conversion of fluorescent protein EosFP. *Proc. Natl. Acad. Sci. USA* **102**, 9156–9159.
68. Andresen, M., Stiel, A. C., Trowitzsch, S., Weber, G., Eggeling, C., Wahl, M. C., Hell, S. W., and Jakobs, S. (2007) Structural basis for reversible photoswitching in Dronpa. *Proc. Natl. Acad. Sci. USA* **104**, 13005–13009.
69. Henderson, J. N., Ai, H. W., Campbell, R. E., and Remington, S. J. (2007) Structural basis for reversible photobleaching of a green fluorescent protein homologue. *Proc. Natl. Acad. Sci. USA* **104**, 6672–6677.
70. Subach, F. V., Patterson, G. H., Manley, S., Gillette, J. M., Lippincott-Schwartz, J., and Verkhusha, V. V. (2009) Photoactivatable mCherry for high-resolution two-color fluorescence microscopy. *Nat. Methods* **6**, 311–311.
71. Kremers, G. J., Hazelwood, K. L., Murphy, C. S., Davidson, M. W., and Piston, D. W. (2009) Photoconversion in orange and red fluorescent proteins. *Nat. Methods* **6**, 355–U355.
72. Stiel, A. C., Trowitzsch, S., Weber, G., Andresen, M., Eggeling, C., Hell, S. W., Jakobs, S., and Wahl, M. C. (2007) 1.8 A bright-state structure of the reversibly switchable fluorescent protein Dronpa guides the generation of fast switching variants. *Biochem. J.* **402**, 35–42.
73. Ando, R., Mizuno, H., and Miyawaki, A. (2004) Regulated fast nucleocytoplasmic shuttling observed by reversible protein highlighting. *Science* **306**, 1370–1373.
74. Vogt, A., D'Angelo, C., Oswald, F., Denzel, A., Mazel, C. H., Matz, M., Ivanchenko, S., Nienhaus, G. U., and Wiedenmann, J. A green fluorescent protein with photoswitchable emission from the deep sea. *PLoS ONE*, 3(11): e3766. doi: 10.1371/journal.pone.0003766.
75. Chudakov, D. M., Verkhusha, V. V., Staroverov, D. B., Souslova, E. A., Lukyanov, S., and Lukyanov, K. A. (2004) Photoswitchable cyan fluorescent protein for protein tracking. *Nat. Biotechnol.* **22**, 1435–1439.
76. Tsutsui, H., Karasawa, S., Shimizu, H., Nukina, N., and Miyawaki, A. (2005) Semi-rational engineering of a coral fluorescent protein into an efficient highlighter. *EMBO. Rep.* **6**, 233–238.
77. Gurskaya, N. G., Verkhusha, V. V., Shcheglov, A. S., Staroverov, D. B., Chepurnykh, T. V., Fradkov, A. F., Lukyanov, S., and Lukyanov, K. A. (2006) Engineering of a monomeric green-to-red photoactivatable fluorescent protein induced by blue light. *Nat. Biotechnol.* **24**, 461–465.
78. Habuchi, S., Tsutsui, H., Kochaniak, A. B., Miyawaki, A., and Van Oijen, A. M. (2008) mKikGR, a monomeric photoswitchable fluorescent protein. *PLoS ONE* **3**, e3944.
79. Nienhaus, G. U., Nienhaus, K., Holzle, A., Ivanchenko, S., Red, F., Oswald, F., Wolff, M., Schmitt, F., Rocker, C., Vallone, B., Weidemann, W., Heilker, R., Nar, H., and Wiedenmann, J. (2006) Photoconvertible fluorescent protein EosFP: biophysical properties and cell biology applications. *Photochem. Photobiol.* **82**, 351–358.
80. Mckinney, S. A., Murphy, C. S., Hazelwood, K. L., Davidson, M. W., and Looger, L. L. (2009) A bright and photostable photoconvertible fluorescent protein. *Nat. Methods* **6**, 131–133.
81. Stiel, A. C., Andresen, M., Bock, H., Hilbert, M., Schilde, J., Schonle, A., Eggeling, C., Egner, A., Hell, S. W., and Jakobs, S. (2008) Generation of monomeric reversibly switchable red fluorescent proteins for far-field fluorescence nanoscopy. *Biophys. J.* **95**, 2989–2997.
82. Wacker, S. A., Oswald, F., Wiedenmann, J., and Knochel, W. (2007) A green to red photoconvertible protein as an analyzing tool for early vertebrate development. *Dev. Dyn.* **236**, 473–480.
83. Ivanchenko, S., Röcker, C., Oswald, F., Wiedenmann, J., and Nienhaus, G. U. (2005) Targeted green-red photoconversion of EosFP, a fluorescent marker protein. *J. Biol. Phys.* **31**, 249–259.
84. Shroff, H., Galbraith, C. G., Galbraith, J. A., White, H., Gillette, J., Olenych, S., Davidson, M. W., and Betzig, E. (2007) Dual-color superresolution imaging of genetically expressed probes within individual adhesion complexes. *Proc. Natl. Acad. Sci. USA* **104**, 20308–20313.
85. Betzig, E., Patterson, G. H., Sougrat, R., Lindwasser, O. W., Olenych, S., Bonifacino, J. S., Davidson, M. W., Lippincott-Schwartz, J., and Hess, H. F. (2006) Imaging intracellular fluorescent proteins at nanometer resolution. *Science* **313**, 1642–1645.
86. Hess, S. T., Girirajan, T. P., and Mason, M. D. (2006) Ultra-high resolution imaging by fluorescence photoactivation localization microscopy. *Biophys. J.* **91**, 4258–4272.
87. Egner, A., Geisler, C., Von Middendorff, C., Bock, H., Wenzel, D., Medda, R., Andresen, M., Stiel, A. C., Jakobs, S., Eggeling, C., Schonle, A., and Hell, S. W. (2007) Fluorescence nanoscopy in whole cells by asynchronous localization of photoswitching emitters. *Biophys. J.* **93**, 3285–3290.
88. Hell, S. W. (2007) Far-field optical nanoscopy. *Science* **316**, 1153–1158.
89. Andresen, M., Stiel, A. C., Folling, J., Wenzel, D., Schonle, A., Egner, A., Eggeling, C., Hell, S. W., and Jakobs, S. (2008) Photoswitchable fluorescent proteins enable monochromatic multilabel imaging and dual color fluorescence nanoscopy. *Nat. Biotech.* **26**, 1035–1040.
90. Baird, G. S., Zacharias, D. A., and Tsien, R. Y. (2000) Biochemistry, mutagenesis, and oligomerization of DsRed, a red fluorescent protein from coral. *Proc. Natl. Acad. Sci. USA* **97**, 11984–11989.
91. Karasawa, S., Araki, T., Nagai, T., Mizuno, H., and Miyawaki, A. (2004) Cyan-emitting and orange-emitting fluorescent proteins as a donor/acceptor pair for fluorescence resonance energy transfer. *Biochem. J.* **381**, 307–312.
92. Nienhaus, K., Renzi, F., Vallone, B., Wiedenmann, J., and Nienhaus, G. U. (2006) Exploring chromophore-protein interactions in fluorescent protein cmFP512 from *Cerianthus membranaceus*: x-ray structure analysis and optical spectroscopy. *Biochemistry* **45**, 12942–12953.
93. Zacharias, D. A. (2002) Sticky caveats in an otherwise glowing report: oligomerizing fluorescent proteins and their use in cell biology. *Sci. STKE. 2002*, PE23.
94. Prescott, M., Ling, M., Beddoe, T., Oakley, A. J., Dove, S., Hoegh-Guldberg, O., Devenish, R. J., and Rossjohn, J. (2003) The 2.2 A crystal structure of a pocilloporin pigment reveals a nonplanar chromophore conformation. *Structure* **11**, 275–284.
95. Campbell, R. E., Tour, O., Palmer, A. E., Steinbach, P. A., Baird, G. S., Zacharias, D. A., and Tsien, R. Y. (2002) A monomeric red fluorescent protein. *Proc. Natl. Acad. Sci. USA* **99**, 7877–7882.
96. Katayama, H., Yamamoto, A., Mizushima, N., Yoshimori, T., and Miyawaki, A. (2008) GFP-like proteins stably accumulate in lysosomes. *Cell Struct. Funct.* **33**, 1–12.
97. Lauf, U., Lopez, P., and Falk, M. M. (2001) Expression of fluorescently tagged connexins: a novel approach to rescue function of oligomeric DsRed-tagged proteins. *FEBS. Lett.* **498**, 11–15.
98. Tao, W., Evans, B. G., Yao, J., Cooper, S., Cornetta, K., Ballas, C. B., Hangoc, G., and Broxmeyer, H. E. (2007) Enhanced green fluorescent protein is a nearly ideal long-term expression tracer for hematopoietic

stem cells, whereas DsRed-express fluorescent protein is not. *Stem Cells* **25**, 670–678.

99. Huang, J., Zhou, W., Watson, A. M., Jan, Y.-N., and Hong, Y. (2008) Efficient ends-out gene targeting in *Drosophila*. *Genetics* **180**, 703–707.
100. Schenkel, M., Sinclair, A., Johnstone, D., Bewley, J. D., and Mathur, J. (2008) Visualizing the actin cytoskeleton in living plant cells using a photo-convertible mEos::FABD-mTn fluorescent fusion protein. *Plant Methods* **4**, 21.
101. Morys, M. and Berger, D. (1993) Accurate measurements of biologically effective ultraviolet radiation. *Proc. SPIE.* **2049**, 152–161.
102. Setlow, R. B., Grist, E., Thompson, K., and Woodhead, A. D. (1993) Wavelengths effective in induction of malignant melanoma. *Proc. Natl. Acad. Sci. USA* **90**, 6666–6670.
103. Rózanowska, M., Jarvis-Evans, J., Korytowski, W., Boulton, M. E., Burke, J. M., and Sarna, T. (1995) Blue light-induced reactivity of retinal age pigment. *J. Biol. Chem.* **270**, 18825–18830.
104. Adam, V., Nienhaus, K., Bourgeois, D., and Nienhaus, G. U. (2009) Structural basis of enhanced photoconversion yield in green fluorescent protein-like protein dendra2. *Biochemistry* **48**, 4905–4915.
105. Wiedenmann, J., and Nienhaus, G. U. Savitsky, A. P. and Wachter, R., eds. (2006) Photoactivation in green to red converting EosFP and other fluorescent proteins from the GFP family. In: Genetically Engineered Probes for Biomedical Applications. Savitsky AP, Wachter RM (eds) Proceedings of SPIE, San Jose, CA, USA, Vol. 6098, p. 1–9. doi: 10.1117/12.657565, *Proc. SPIE.* 609801.
106. Kawano, H., Kogure, T., Abe, Y., Mizuno, H., and Miyawaki, A. (2008) Two-photon dual-color imaging using fluorescent proteins. *Nat. Methods* **5**, 373–374.
107. Ivanchenko, S., Glaschick, S., Rocker, C., Oswald, F., Wiedenmann, J., and Nienhaus, G. U. (2007) Two-photon excitation and photoconversion of EosFP in dual-color 4Pi confocal microscopy. *Biophys. J.* **92**, 4451–4457.
108. Drobizhev, M., Tillo, S., Makarov, N. S., Hughes, T. E., and Rebane, A. (2009) Absolute two-photon absorption spectra and two-photon brightness of orange and red fluorescent proteins. *J. Phys. Chem. B* **113**, 855–859.
109. Bulina, M. E., Lukyanov, K. A., Britanova, O. V., Onichtchouk, D., Lukyanov, S., and Chudakov, D. M. (2006) Chromophore-assisted light inactivation (CALI) using the phototoxic fluorescent protein KillerRed. *Nat. Protoc.* **1**, 947–953.
110. Tour, O., Meijer, R. M., Zacharias, D. A., Adams, S. R., and Tsien, R. Y. (2003) Genetically targeted chromophore-assisted light inactivation. *Nat. Biotechnol.* **21**, 1505–1508.
111. Link, C. D., Fonte, V., Hiester, B., Yerg, J., Ferguson, J., Csontos, S., Silverman, M. A., and Stein, G. H. (2006) Conversion of green fluorescent protein into a toxic, aggregation-prone protein by C-terminal addition of a short peptide. *J. Biol. Chem.* **281**, 1808–1816.
112. Luche, H., Weber, O., Rao, T. N., Blum, C., and Fehling, H. J. (2007) Faithful activation of an extra-bright red fluorescent protein in "knock-in" Cre-reporter mice ideally suited for lineage tracing studies. *Eur. J. Immunol.* **37**, 43–53.
113. D'Angelo, C., Denzel, A., Vogt, A., Matz, M. V., Oswald, F., Salih, A., Nienhaus, G. U., and Wiedenmann, J. (2008) Blue light regulation of host pigment in reef-building corals. *Mar. Ecol. Prog. Ser.* **364**, 97–106.
114. Mustafa, H., Strasser, B., Rauth, S., Irving, R. A., and Wark, K. L. (2006) Identification of a functional nuclear export signal in the green fluorescent protein asFP499. *Biochem. Biophys. Res. Commun.* **342**, 1178–1182.